Journal of
Materials Chemistry A

Accepted Manuscript

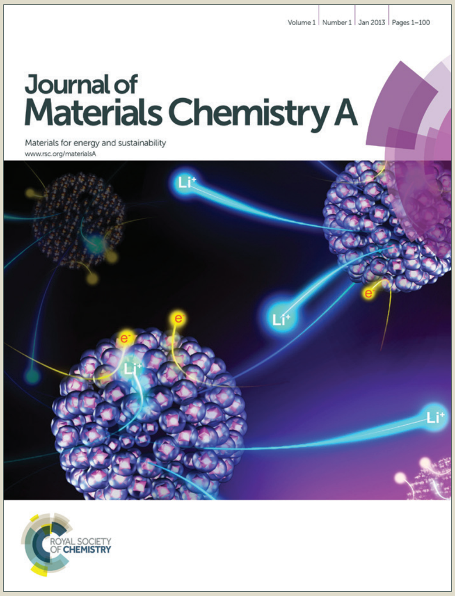

ROYAL SOCIETY
OF **CHEMISTRY**

www.rsc.org/materialsA

Title Page

Title

NiCo$_2$O$_4$-based Materials for Electrochemical Supercapacitor

Author names and affiliations

Zhibin Wu, Yirong Zhu, Xiaobo Ji*

Department of Chemistry and Chemical Engineering, Central South University, Changsha, 410083, China.

Corresponding author

Xiaobo Ji*

Department of Chemistry and Chemical Engineering, Central South University, Changsha, 410083, China.

Email address: xji.csu.edu@ gmail.com

Tel: +86 731-88879616

Fax: +86 731- 88879616

Abstract

With advanced electrochemical performance, nickel cobaltite ($NiCo_2O_4$) has become a new class of energy storage material for electrochemical supercapacitors, devoting to relieve the pressure of energy crisis and environmental pollution. It possesses richer electroactive sites and at least two magnitudes higher electrical conductivity than that of NiO and Co_3O_4, exhibiting not only large power density, but high energy density up to 35 Wh kg^{-1}. Furthermore, it shows comparable capacitive performances with noble metal oxides of RuO_2, but with much lower cost and more abundant resources. This feature article briefly analyses energy storage mechanism of $NiCo_2O_4$, summaries the methodologies and nanostructures prospering in recent years, and points out the potential problems and prospects the wonderful future utilizing $NiCo_2O_4$-based materials as supercapacitor electrodes. Additionally, composite electrodes based on nickel cobaltite are also elaborated with great interest. Since the pioneering work of Hu and his group in 2010, numerous research followed have also demonstrated $NiCo_2O_4$ electrodes to be remarkable supercapacitive performances, however, more specialized work should be done to further develop the potential of this novel electrode material so as to realize the massive commercial application.

Keywords

Nickel cobaltite; electrochemical supercapacitor; pseudocapacitance; energy storage

1. Introduction

With the further depletion of fossil fuels and considerable concern about the global environmental impacts of conventional energy technologies, there comes an urgent need for the development of new energy sources and new technologies associated with energy conversion and storage.[1,2] In the recent decades, the growing interests in hybrid electric vehicles and portable electronic devices have created a seemingly insatiable demand for energy storage, which have also presented great challenges to the enhancement of electrochemical performances.[3,4] In this context, electrochemical supercapacitors, as a type of special and novel storage device devoting to meet the ever-growing consumption demands and alleviate the energy crisis, have attracted great research attention mainly due to their high power density, long cycle life and rapid recharge capability, as well as bridging function for the power and energy gaps between batteries and traditional dielectric capacitors.[5-7] Note that electrode materials have become the core competence for supercapacitors and they can be typically divided into three types including carbon materials, conducting polymers and transition metal oxides. Carbon materials with low cost, extremely developed surface area (up to 3000 m^2 g^{-1}), good electrical conductivity and chemical stability seem to be ideal materials for electrical double-layer capacitors, but it usually suffers from low specific capacitance (commonly lower than 400 F g^{-1}).[8-12] While conducting polymers have higher specific capacitance (usually lower than 530 F g^{-1}) and excellent intrinsic conductivity, however, their cycle-life is extremely poor because of its substantial expansion and contraction during the charging-discharging process.[13,14] Compared with the two types mentioned above, transition metal oxides usually possess multiple oxidation states that are in favor of fast redox reaction resulting in a much higher specific capacitance.[15-17] Due to the intrinsic low electronic conductivities of these transition metal oxides with band gaps ranging from 3 to 4 eV, one cannot guarantee their striking electrochemical performance, especially at ultrahigh rates, unless combined with other good conductive materials.[18-20] In recent years, transition metal oxides such as RuO_2,[21,22] NiO,[23,24] Co_3O_4,[25,26] MnO_2,[27,28] have been widely investigated as promising electrode materials for supercapacitors. Among them, RuO_2 exhibits the best electrochemical performances because of the relatively better conductivity, highly reversible charging-discharging properties and large specific capacitance (as high as 1580 F g^{-1}).[29] Nevertheless, its large-scale application is greatly limited by its high cost and toxic nature. The applications of other metal oxides are mainly restricted by their poor electrical conductivity and low energy density. Therefore, it is imperative to develop alternative electrode materials of low-cost, environmental friendliness and superior electrochemical performances.[30,31]

Nickel cobaltite ($NiCo_2O_4$) possesses better electrochemical activity and at least two orders of magnitude higher electrical conductivity than pure Co_3O_4 and NiO, which can exhibit an outstanding specific capacitance of 1400 F g^{-1} at a sweep rate of 25 mV s^{-1} in a 1 M NaOH solution within a potential window of 0.04 to 0.52 V as reported by Hu and his group in 2010.[32] The electrical conductivity deduced from **Figure 1** is in sequence of $NiCo_2O_4 > NiO > Co_3O_4$, and lots of work also demonstrated that nickel cobaltite has a much lower resistance than nickel oxides and cobalt oxides.[33-35] It is believed that the redox reactions offered by nickel cobaltite, including contributions from both nickel and cobalt ions, are richer than those of the monometallic nickel oxides and cobalt oxides. More importantly, multiple oxidation states and various nanostructures can also enable rich redox reactions for spinel nickel cobaltite to store more charges.[32,36-38] Last but not least, there are abundant nickel and cobalt elements on the earth, and it seems to be a promising opportunity for nickel cobaltite to be widely applied and industrialized as electrode material due to its low-cost and environmental-friendly benefit.[39,40] To some extent, $NiCo_2O_4$ is playing an important role in complementing or replacing electrode materials based on NiO, Co_3O_4 and RuO_2 in energy storage field. A Ragone plot (**Figure 2**) derived from $NiCo_2O_4$-based asymmetrical supercapacitors' work illustrates energy density against power density for current booming development.

To date, there are some reviews that cover different topics in the development of transition metal oxides.[30,41-43] However, to the best of our knowledge, there is no review dedicated to the development of $NiCo_2O_4$-based pseudocapacitors. In this paper, we categorize and review the most important related works and achievements of $NiCo_2O_4$-based pseudocapacitors published in the last few years. Firstly, possible energy storage mechanism of $NiCo_2O_4$ as electrode material is discussed. Then, we review the synthetic methods of $NiCo_2O_4$-based materials, mainly including sol-gel method, hydrothermal synthesis and electrodeposition process. After that, the assemblies of $NiCo_2O_4$-based electrode materials including pure $NiCo_2O_4$ and $NiCo_2O_4$-based composite materials are summarized. In the end, we prospect the current challenges and future strategies for this particular material.

2. Energy storage mechanism of $NiCo_2O_4$

As a novel electrode material for pseudocapacitor, nickel cobaltite stores its charges both on the surface and in the bulk near the surface of the solid electrode where the electrochemical processes occur.[44] It possesses a ferrimagnetic cubic spinel structure with multiple redox states and good electrical conductivity as a P-type semiconductor with the band gap of 2.1 eV.[45] Note that $NiCo_2O_4$ adopts a spinel structure in which all the nickel cations occupy the octahedral interstices, whereas the cobalt cations are distributing among the tetrahedral and octahedral interstices.[46] And it has been reported that the oxidation state distributions of nickel cobaltite are the matter of some uncertainties, so its general formula can be expressed as $Co^{2+}_{1-x}Co^{3+}_{x}[Co^{3+}Ni^{2+}_{x}Ni^{3+}_{1-x}]O_4, 0 \le x \le 1$. (cations preceding the brackets are taken to be in tetrahedral interstices and those within the brackets are in octahedral interstices).[36,47-49] Note that "x" could be 0, 0.1, 0.2, 0.65, 1 and so on, as proposed in literature.[50] That is to say, $NiCo_2O_4$ has the spinel minerals generic formula of AB_2O_4 with a mixed valence compound. As shown in **Figure 3**, oxygen atoms in a spinel are arranged in a cubic close-packed structure, and the cations of A and B occupy some or all of the octahedral and tetrahedral sites in the lattice.[41,51] From another perspective, $NiCo_2O_4$ may be simply regarded as a nickel atom substituting one of the cobalt atoms in Co_3O_4. What makes the difference between $NiCo_2O_4$ and Co_3O_4 in physicochemical properties is the insertion of nickel atom which has the similar size with cobalt atom that causes the subtle change of crystal structures in which the defects may take some unexpected effects on electrochemical performances. However, more details and evidences are worth being explored and discovered in the future.

As reported in some work, [32,52,53] nickel cobaltite shows a potential window of 0 to 0.55 V in an alkaline solution and its pseudo-capacitive behavior in the alkaline electrolyte can be described by the following equations:

$$NiCo_2O_4 + OH^- + H_2O \rightleftharpoons NiOOH + 2CoOOH + e^- \qquad (1)$$

$$CoOOH + OH^- \rightleftharpoons CoO_2 + H_2O + e^- \qquad (2)$$

More details are illustrated in **Figure 4**. It is noteworthy that, in the charging-discharging process, there exist valence state changes of Co^{3+}/Co^{4+} as well as M^{2+}/M^{3+}(M=Co or Ni) on the surface of the electrode materials, where fast and reversible faradaic reactions occur.[34,54,55] The electrochemical redox potentials of M^{2+}/M^{3+} and Co^{3+}/Co^{4+} transitions are so close that the redox peaks observed is becoming an overlapping one as reported. Moreover, it should be noting that the metal oxides possess not only double layer capacitance but also high pseudo capacitance (typically 10 ~ 100 times higher than double layer capacitance),[44] therefore, the double layer capacitances shown by CV curves for the electrodes are relatively too small to be observed. Unfortunately, the theoretical capacitance of nickel cobaltite as electrode material for supercapacitor has not been calculated yet and we do hope that more detailed evidences can be put forward to clarify the storage mechanism of this unique material. The capacity retention rate is another important index to evaluate the supercapacitive performance, intriguingly, the specific capacitance of $NiCo_2O_4$ is observed to rise up to some extent after several hundred cycles in some work attributing to their unique morphologies and the process of activation.[56,57] Thus, it seems that the mass loading of $NiCo_2O_4$ has a great influence on the supercapacitive performance. Aiming at storing more charges and reducing the impact of mass loading, novel structures with large specific surface area, unique morphology and well-defined size are crucial to be fabricated to make full use of this material.

3. Synthetic strategies for $NiCo_2O_4$

Although great progress has been made in synthesizing $NiCo_2O_4$ nanoparticles for supercapacitors, most work has solely been researched as no review highlights this novel electrode material. In this section, we put forward a comprehensive overview of synthetic strategies for $NiCo_2O_4$. These methods can be typically divided into three categories: （1） sol-gel method, （2） hydrothermal synthesis, （3）electrodeposition process. Generally speaking, the synthetic route of $NiCo_2O_4$ nanoparticles can be thought of as the formation of precursor followed by a calcinating process. The three primarily methods are summarized in **Figure 5** and discussed in detail below, and other methods are also briefly mentioned.

3.1 Sol-gel method

In general, the sol–gel method can be briefly defined as the conversion of a precursor solution into an inorganic solid by chemical ways.[58] Herein, the precursor solution consists of either an inorganic metal salt or a metal organic species, while nickel and cobalt halides, acetates, nitrates are typically used here for preparing $NiCo_2O_4$.[59,60] It is well known that the sol–gel method is simple and cheap with products of high purity, homogeneity and porosity, mainly including four steps: (1) preparation of the precursor solutions (2) formation of the intermediates as sol (3) transformation from sol to gel (4) calcination. No doubt, surfactants, solvents, reaction time and temperature are the key regulatory factors to get appropriate structures with remarkable electrochemical performances.[58]

Hu and his co-workers[32] first reported the preparation of $NiCo_2O_4$ aerogels via an epoxide-driven sol–gel process in 2010, which exhibited an ultrahigh specific capacitance of 1400 F g^{-1} under a mass loading of 0.4 mg cm^{-2}. The majority of the pores were falling in the optimal sizes of 2–5 nm for supercapacitor applications and the product aerogels were of excellent reversibility and cycle stability. Since this pioneering work, several researches have been devoted on this sol-gel approach.[61-65] The typical preparation process is illustrated in **Figure 5**a and the mechanism of gelation can be explained as the following reaction sequence where M represents nickel or cobalt ions, A^- represents Cl^- or NO_3^- ions.[63]

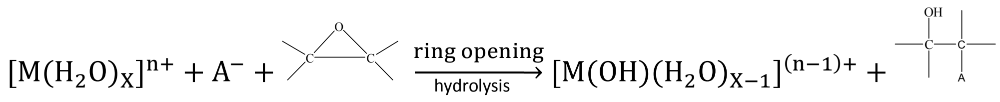

Additionally, Wu *et al.*[62] pointed out that the initial molar concentration of reactants, reaction time and solvent species involved are crucial for preparing the target products. By using citric acid as the chelating ligand and H_2O-DMF as solvent via a facile sol-gel process, the submicron-sized $NiCo_2O_4$ particles exhibited a specific capacitance of 217 F g^{-1} with high mass loading of 5.6 mg cm^{-2}. While Kong *et al.*[61]

developed a sol-gel process by adding different surfactants, such as hexadecyltrimethylammonium bromide (CTAB) and polyvinyl alcohol (PVA), to control the microstructure and surface morphology of $NiCo_2O_4$ nanoparticles. The product modified by CTAB shows the highest specific capacitance of 1440 F g^{-1} at a current density of 5 mA cm^{-2}. Extensive work is on-going via a sol-gel process to prepare a better modality of $NiCo_2O_4$ so as to achieve a higher specific capacitance and a longer cycle life. It has been proved to be a remarkable way indeed to synthesize $NiCo_2O_4$ electrode materials with low-cost and high electrochemical performances.

3.2 Hydrothermal synthesis

Hydrothermal/solvothermal synthesis refers to the heterogeneous chemical reactions in a sealed heated solution to dissolve and recrystallize materials above ambient temperature and pressure conditions.[66] Hydrothermal synthesis and solvothermal synthesis are similar synthetic strategies that are distinct from whether the solution is aqueous or not. For convenience and habit, we call them hydrothermal synthesis uniformly. In general，the precursors of $NiCo_2O_4$ are formed by a combination of reaction substances being heated in a sealed Teflon-lined stainless steel autoclave. As the most common method of synthesizing nickel cobaltite, it is advantageous to form highly monodispersed nanoparticles with a control over size and morphology.[67]

A huge number of groups have made attempts to optimize the reaction conditions and form special morphologies so as to enhance the electrochemical performances of $NiCo_2O_4$ electrodes.[53,56,68-72] For example, Chen *et al.*[53] reported that a 3D hierarchical $NiCo_2O_4$ nanosheet-nanowire cluster arrays were manufactured via a facile hydrothermal method, exhibiting an ultrahigh specific capacitance of 2000 F g^{-1} at 10 A g^{-1} with 93.8 % retention (more than 10000 cycles) and a high-power density of 26.1 kW kg^{-1} at a current density of 80 A g^{-1}. As illustrated in **Figure 5**b, the process is based on Ni-Co nitrates induced by NH_4F and urea being heated in a sealed Teflon-lined stainless steel autoclave at 100℃ for 5 h. At the same time, both the mechanism of morphology evolution and the impact of the amount of NH_4F have also been investigated that is shown in **Figure 6**. Besides, Zou *et al.*[68] also reported a facile hydrothermal method that successfully grew 3D $NiCo_2O_4$ micro-spheres constructed by radial chain-like $NiCo_2O_4$ nanowires with different exposed crystal planes, demonstrating high specific capacitance (1284 F g^{-1} at 2 A g^{-1}), good rate capability, and excellent cycling stability (only 2.5 % loss after 3000 cycles). It was proposed that the chain-like nanowires with different exposed crystal planes exhibited higher electronic conductivity than other mesoporous $NiCo_2O_4$ nanostructures. In comparison, solvothermal method just occurs in non-aqueous solvents such as ethanol and ethylene glycol. Very recently, the 3D flower-like $NiCo_2O_4$ hierarchitectures have been fabricated by An *et al.*[56] via a solvothermal method using polyvinylpyrrolidone (PVP) as the structure-directing agent in a polytetrafluoroethylene (PTFE) reaction environment followed by a simple thermal annealing treatment, displaying a large surface specific area of 212.6 m^2 g^{-1} and a high specific capacitance of 1191.2 F g^{-1} at current densities of 1 A g^{-1}, however, it suffered from a relatively poor cycling performance due to the electric isolation caused by collapse of the nanosheets.

3.3 Electrodeposition process

The electrodeposition process occurs in the electrolysis of plating solutions where micron- or submicron-size particles are suspended, and variable amounts of these particles are embedded in the electrochemically produced solid phase with special properties.[73] As illustrated in **Figure 5**c, the process can be divided into three steps: (1) formation of precursor solution; (2) co-electrodeposition of nanoparticles; (3) thermal decomposition. Due to cooperative formation mechanism of the composite electrode, as a general rule, ultrahigh specific capacitances and good cycling performances are achieved through this novel method.[36,74-78]

For instance, Du *et al.*[77] successfully electrodeposited $NiCo_2O_4$ nanosheet arrays onto flexible carbon fabric (CF), which displayed high specific capacitance of 2658 F g^{-1} (2 A g^{-1}), good rate property and superior cycling life. Note that carbon fabric is an ideal conductive substrate for directly growing active materials owing to its superior electrical conductivity, good flexibility and high mechanical strength, through which we can fabricate some distinctive flexible supercapacitors or lithium ion batteries. Moreover, Lou and his coworkers[36] reported the synthesis involving the co-electrodeposition of a bimetallic (Ni, Co) hydroxide precursor on a Ni foam and subsequently thermal transformation to spinel mesoporous $NiCo_2O_4$, and the electrode exhibited an ultrahigh specific capacitance of 1450 F g^{-1} even at a very high current density of 20 A g^{-1}. The sizes of inter-particle mesopores were ranged from 2 to 5 nm, which were important indeed to facilitate the mass transport of electrolytes within the electrodes for fast redox reactions and double-layer charging-discharging. Composite electrodes such as $Ni(OH)_2@NiCo_2O_4$[75] and $Co_3O_4@NiCo_2O_4$[74] via the electrodeposition method were also reported in literature. And the formation process of the nanoforest of hierarchical $Co_3O_4@NiCo_2O_4$ nanowire arrays is elaborated in **Figure 7** as a typical example.

Electrodeposition process is the most widely used method to form composite electrodes with different nanomaterials. It is very important to choose the befitting materials that possess good electrical conductivity or unique nanostructure to assist the target material in pursuing for much better electrochemical performances. However, the ambiguous relationship between the composite structures and electrochemical performances has not been clarified yet.

3.4 Summary of synthesis methods

The fundamentals and technique approaches in synthesizing $NiCo_2O_4$-based electrodes have been summarized in this chapter. Three groups of synthesis methods, including sol–gel method, hydrothermal synthesis and electrochemical deposition, have been reviewed and discussed in details. In addition, other methods, such as co-precipitation method, template approach, chemical bath deposition, microwave and sonochemical technique, are also simply mentioned below, which are not widely used or just assistant measures for fabricating electrodes based on $NiCo_2O_4$ material.

As elaborated above, all of the three major methods are distinctive. The sol-gel method tends to acquire nanoparticles of high purity, homogeneity and porosity. And the hydrothermal synthesis is controllable of size and nanostructure by adjusting temperature parameters or types and concentration of auxiliaries. By contrast, the electrodeposition process has some distinct advantages to deposit $NiCo_2O_4$ onto various conductive substrates such as nickel foams and carbon textiles and to combine $NiCo_2O_4$ with some other excellent materials that show intriguing synergistic effect, which can be manipulated through adjusting solution concentration, solution pH value, and applied overpotential or current density.

Herein, the following examples are constructed only for the purpose of comprehensively illustrating the diversity and novelty of processes as reported. Recently, it has been reported that microwave technique has been used to help prepare $NiCo_2O_4$ electrodes for supercapacitors. What is more, the microwave-assisted process has been demonstrated to be advantageous to extremely fast kinetics of crystallization, very rapid heating to the required temperature and possible formation of new meta-stable phases, which facilitate to tune the crystal size and phase transformation degree of binary Ni-Co precursors.[79,80] As a flexible and efficient approach, the template approach, using silica spheres[81] and sodium dodecyl sulfate[82] as templates, has been used to synthesize hierarchical mesoporous hollow $NiCo_2O_4$ sub-microspheres and hexagonal mesoporous $NiCo_2O_4$ for supercapacitor electrodes, respectively. Both of them show remarkable electrochemical performances. Note that surfactants,[19,50,56,61,62] such as hexadecyltrimethylammonium bromide (CTAB), polyvinyl alcohol (PVA), and citric acid, have also been studied extensively, which contributes to acquire unique morphologies and excellent electrochemical performances. Besides, sonochemical precipitation technique,[83] chemical bath deposition,[84] co-precipitation method[85,86] and single-spinneret electrospinning technique[87] have also been utilized to synthesize $NiCo_2O_4$ nanostructures for supercapacitors. They deserve a mention equally and the bibliography will point to detailed references for those wishing this level of detail.

4. Assemblies of $NiCo_2O_4$-based materials

In order to further improve the electrochemical performances of $NiCo_2O_4$-based electrodes, numerous works have been conducted on the design of the electrode material as shown in **Figure 8**, including assemblies of various structures and incorporations of novel substances.

For pure nickel cobaltite material, structural evolution from simple to complex is of great significance because the special nanostructures could notably influence the performance of materials. At present, simple nanostructures such as nanotubes, nanowires and nanosheets are primarily built and complex nanostructures are rarely created for nickel cobaltite. Multilevel interior structures such as core-hollow shell structured nanospheres have many advantages over simple nanostructures. It facilitates to effectively prevent the interior particles from aggregating and make the interior particles expose its active surface sufficiently.[88] Of course, more active sites and better mechanical properties will also be obtained.

For $NiCo_2O_4$-based composite material, it is crucial to combine proper materials with $NiCo_2O_4$ for a complete synergy of action. As for the realizing level of the synergistic effect, it depends not only on the types of material to be combined but also on the characteristics of structures to be built. It has been reported that spinel $NiCo_2O_4$ has a big advantage over NiO and Co_3O_4 on electrical conductivity as mentioned above,[32-35] however, it shows no obvious superiority when compared with conductors as almost all the transition metal oxides are semiconducting in nature. Note that the relatively large charge-transfer resistance limits the enhancement of power density of $NiCo_2O_4$ electrodes. Incorporations of other materials that possess good electrical conductivity into $NiCo_2O_4$ nanostructures will introduce more defects and charge carriers and it is a potential route to enhance the electrical conductivity and charge-storage capability of nickel cobaltite.

The other consideration for alleviating the relatively poor electronic conductivity of $NiCo_2O_4$ electrodes is to tailor the electrode architecture by applying an ultrathin layer of $NiCo_2O_4$ on the surface of a porous, high surface area and electronically conducting structure, including nickel foams, carbon textiles and flexible graphite paper, etc,[71,89] to shorten the electron transport distance. The electrode architectures can provide fast electron transport by direct connection to the growth substrate, producing good electrochemical performances without sacrificing the mass-loading of the $NiCo_2O_4$ phase.

4.1 Pure $NiCo_2O_4$ materials

Homogenous $NiCo_2O_4$ materials with diverse structures are prepared, which show various performances that attract us a lot. Herein, we briefly review the current morphology progress and some conclusions derived from **Table 1**.

There are a number of nanostructures reported in the recent literatures, including one-dimensional (1D), two-dimensional (2D) and three-dimensional (3D) nanostructures. In general, 3D nanostructures have an advantage over 1D and 2D nanostructures in energy storage due to the following advantages: First, it provides the large volume of a 3D continuous electron transport channels for electrolyte ion accumulation by acting as an ion reservoir. Second, convenient electrolyte penetration–diffusion and large electrode–electrolyte interface are obtained simultaneously. Third, it tends to possess higher electrical conductivity and better structural mechanical stability, resulting in superior electrochemical performances.[19,53,90,91] As a representative figure, the TEM photos and the charge storage advantages of the 3D interconnected hierarchical porous network-like $NiCo_2O_4$ are illustrated in **Figure 9**. The unique network-like $NiCo_2O_4$ electrode features a good cyclability and a specific capacitance of 587 F g^{-1} at 2 A g^{-1} (518 F g^{-1} at 16 A g^{-1}) with a loading mass of 5 mg cm^{-2}.[19] Besides, it has been reported that $NiCo_2O_4$ nanowall-network structure delivers a specific capacitance of 1225 F g^{-1} at 5 A g^{-1} compared to $NiCo_2O_4$ nanoflakes of 844 Fg^{-1} at 1 A g^{-1} with the same loading mass.[91] Similarly, the 3D hierarchical NH_4F-induced $NiCo_2O_4$ nanosheet–nanowire cluster arrays reported by Chen *et al.* also show better electrochemical performances than the nanowire arrays, which demonstrates the correctness of the hypothesis as well.[53]

In addition, it is apparent that ordered mesoporous nanosheets and nanowire arrays structured nickel cobaltites possess relatively higher capacitances than other 1D and 2D nanostructures. Recent experiments in this area have indicated that ordered mesoporous $NiCo_2O_4$ nanosheets, as illustrated in **Figure 10**a and b, show superior pseudocapacitor performance than that of disordered porous $NiCo_2O_4$.[92,93] To the best of our knowledge, the pseudocapacitive difference is related to the pore geometry, size distribution and specific surface area of $NiCo_2O_4$ nanocrystals. On the one hand, mesoporous feature might possess suitable storage spaces for ions and increasing electroactive sites for redox reaction. On the other hand, ordered feature could provide better mechanical strength and efficient channels for penetration of the electrolyte ions, which is helpful to fast charging-discharging process.

Beyond all that, it is worth highlighting that $NiCo_2O_4$ nanowire arrays supported on Ni foam exhibit superior pseudocapacitor behaviors with specific capacitance of 2681 F g^{-1} at a current density of 2 A g^{-1} with a high loading mass of 3 mg cm^{-2}, owing to its high surface area and shortened ion diffusion path provided by allied nanowire arrays, which has been the highest specific capacitance of pure $NiCo_2O_4$ pseudocapacitors as has been reported so far.[94] As can be seen from **Figure 10**c and d, highly aligned nanowire arrays with lengths of about 3 mm and average diameters of 80–200 nm are grown vertically on the whole Ni foam.

4.2 $NiCo_2O_4$-based composite material

The basic problem in a composite electrode is focused on the material incorporated, which plays the decisive role in enhancing the electrochemical performances. In addition, selecting a proper methodology to build structures with rational design is also vital. At present, a wealth of work in this field has been done as listed in **Table 2** and the following paragraphs will introduce the incorporated materials consisting of carbon materials, transition metal oxides and other substances.

4.2.1 Carbon materials-$NiCo_2O_4$

Carbon materials, such as activated carbons, carbon nanofibres, carbon nanotubes, carbon aerogels, graphenes, ordered mesoporous carbons are typically used for fabricating $NiCo_2O_4$-based composite electrodes due to their outstanding physicochemical properties, including good electrical conductivity, large activated surface areas, strong mechanical strength and high chemical stability.[10] Carbon materials for supercapacitors have been extensively exploited during the last two decades, however, as is well-known that the capacitances of carbon materials are generally much lower than that of transition metal oxides, which limits their practical applications to some extent. Nevertheless, a combination of $NiCo_2O_4$ and carbon materials may make full use of the excellent electrical conductivity and large activated surface areas of carbon materials as well as the ultrahigh specific capacitance of $NiCo_2O_4$. More recently, nickel cobaltite has been successfully deposited into carbon aerogels with a two-step wet chemistry process, showing higher specific capacitances of around 1700 F g^{-1} than that of 1400 F g^{-1} achieved for the $NiCo_2O_4$ aerogels at the same scan rate of 25 mV s^{-1}.[32,95] There are no apparent differences between **Figure 11**a and b, which indicates that the introduction of $NiCo_2O_4$ does not change the essential microstructural characteristics of the carbon aerogel sample. Otherwise, **Figure 11**c and d show the consistent of $NiCo_2O_4$ nanocrystals with a size of 3–5 nm. It is worth mentioning that carbon aerogels are a class of mesoporous nanostructures with high porosities, high specific surface areas, and the 3D-well-connected through pore structures that can efficiently improve the performances of the electrode. Intriguingly, graphene,[96] graphene oxide[97] and reduced graphene oxide[98] are respectively combined with $NiCo_2O_4$ nanoparticles at the nanoscale by different methods, which exhibit various electrochemical performances. The asymmetric supercapacitor consisting of the graphene@$NiCo_2O_4$ nanocomposite (anode) and commercial activated carbon (cathode) deliver an energy density of 7.6 Wh·kg^{-1}at a power density of about 5600 W·kg^{-1} with a mass loading of 10 mg·cm^{-2}, and maintain 102 % of the initial capacitance after 10000 cycles. The graphene skeleton retains a high electrical conductivity even for very thick electrodes and completely prevents cycling-induced degradation. Among the three nanocomposite materials mentioned above, reduced graphene oxide@$NiCo_2O_4$ electrode shows the highest capacitance of 1693 F g^{-1} (1 A g^{-1}) owing to its best synergistic effect derived from nanocomposite structure.

So far, great progress has been made, yet much remains to be done. Most importantly, taking advantage of the high conductivity and high surface area of carbon materials are the key points in fabricating carbon materials@$NiCo_2O_4$ composite electrodes. In addition, fascinating structures and novel allotropes based on carbon, to be discovered in virtue of the advancement of modern nanotechnology, is urgently expected to be combined with $NiCo_2O_4$. In a word, it is carbon materials that provide fast electron transfer and large contact area of electrolyte ions penetration in the hybrid storage system.

4.2.2 Transition metal oxides-$NiCo_2O_4$

Although $NiCo_2O_4$ possesses at least two magnitudes higher conductivity than NiO and Co_3O_4, it is still of great significance to study the effects when they are combined with $NiCo_2O_4$ considering that both NiO and Co_3O_4 are also favorable candidates of high-performance supercapacitor materials in the future. Growing smart integrated architectures with the combination of different types of materials such as MnO_2, NiO, and Co_3O_4 have many competitive advantages including abundant accessible electroactive sites, superior electron collection efficiency, short ion transport pathways, and even fascinating synergetic properties or multifunctionalities of components.[99] For example, Zhang *et al.*[74] have reported that the nanoforest of hierarchical Co_3O_4@$NiCo_2O_4$ nanowire arrays show a promising synergistic effect for supercapacitors with a specific capacitance of 526.7 F g^{-1} (almost 2.5 times as high as that of pristine Co_3O_4) even measured at 20 A g^{-1}. The firstly-grown Co_3O_4 array provides a scaffold for the later $NiCo_2O_4$ growth, decreasing the conventional aggregation and ensuring sufficient ion diffusion. By contrast, the

$NiCo_2O_4$@NiO/carbon cloth-based all-solid state supercapacitor exhibits a high initial discharge capacitance of 1289 F g^{-1} at 33.6 A g^{-1} along with capacity retention of 87.5 % after 5000 cycling.[100] As can be seen in **Figure 12**, large-scale uniform sheet-like NiO nanoparticles prepared by the chemical bath deposition process are successfully in situ grown on the whole framework, forming a conformal coating on the surface of $NiCo_2O_4$ nanowires. Further insight into the detailed microstructure of the core–shell nanowire is elucidated by HRTEM (**Figure 12**d). Interestingly, Liu *et al.*[63] fabricated another NiO@$NiCo_2O_4$@Co_3O_4 composite electrodes via a sol-gel method, which exhibited a higher specific capacitance of 1717 F g^{-1} than sole NiO, $NiCo_2O_4$, and Co_3O_4, owing to the improved electrical conductivity, low crystallinity, and proper mesoporous structure of the composite.

There are many other transition metal oxides such as Mn_3O_4, WO_3, MoO_3, TiO_2, SnO_2, Fe_3O_4, CoO and V_2O_5, and even ternary transition metal oxides remained to be explored by combining with $NiCo_2O_4$ respectively. A wealth of information can be found in literatures, however, it will still take great efforts to study the synergistic effects with a series of experiments aimed at improving the ultimate electrochemical performances.

4.2.3 Other materials-$NiCo_2O_4$

As different kinds of materials have different unique properties, there generate many advanced materials that could be combined with $NiCo_2O_4$. The data consist of hydroxides, carbonates, sulfides and conducting polymers, etc. However, there is almost no research on the methodology that combines $NiCo_2O_4$ nanocrystals with them except hydroxides. In this section, the characteristics and methodologies of metal hydroxides@$NiCo_2O_4$ composite electrode are mainly described. The composite electrode involving the procedure of $Ni(OH)_2$ nanoplates@$NiCo_2O_4$ nanosheets growing on carbon fiber paper shows an ultrahigh specific capacitance of 3250 F g^{-1} (measured at 1.25 A g^{-1}) owing to its short diffusion path lengths that are in favor of the diffusion and migration of electrolyte ions.[75] However, it proves to be very poor cycling stability which dropped over 64 % after 1000 cycles with the rapid decreasing specific surface area. Compared to the composite electrode mentioned above, the composite electrode of $Co_{0.66}Ni_{0.33}(OH)_2$@$NiCo_2O_4$ displays better cycling stability of a total capacitance loss of about 18.7 % after 2000 cycles, maintains high capacitance of 1640 F g^{-1} (measured at 2 A g^{-1}), and offers remarkable specific energy density of 33 Wh/kg and power density of 41.25 kW/kg at high cycling rates (up to 150 mA cm^{-2}). The optimal performance is obtained from systematically investigation on the coating material of $Co_xNi_{1-x}(OH)_2$ with variable ratios of cobalt to nickel[101] and related results are listed in **Figure 13** and **Figure 14**. Note that incorporating metal hydroxides into $NiCo_2O_4$ crystals may be advantageous to further improve the capacitive performance and other materials are expected to apply in the same way.

5. Summary and outlook

Current advancement in methodologies and nanostructures of $NiCo_2O_4$-based pseudocapacitors has been summarized in this feature article. Novel methods and composite structures applied to $NiCo_2O_4$-based electrodes greatly promote the development of power storage device. $NiCo_2O_4$-based materials with fascinating electrochemical performances have been proven to be one of the most promising electrode materials for supercapacitor applications. Its main advantages are the following: good electrical conductivity, rich electroactive centrals, stable spinel structure, and environmentally benign applicability. In this paper, some classical methods, including sol-gel process, hydrothermal synthesis and electrochemical deposition, are illustrated in detail. Besides, various morphologies are also described, which show diverse capacitive performances. Note that uniform and multi-lever particles are advantageous to possess excellent electrochemical properties, and facile and low-cost methods are also pursued by investigators. It is promising that more powerful fabrication methods to be used in designing rational electrodes with outstanding electrochemical performances will be successfully developed. Although the full potential of $NiCo_2O_4$-based pseudocapacitors has not been realized yet, as outlined in the present review, a skeleton structure for future technical advancements has been established. However, there are many problems remained to be settled as mentioned in the following: First and foremost, it is challenging to further explore the mechanism during the charging-discharging process so as to throw light on the rational design of $NiCo_2O_4$-based pseudocapacitors in the future; Secondly, both the theoretical capacitance and the oxidation state distributions of $NiCo_2O_4$ are important indeed to be clarified; Thirdly, systematic research should be focused on removing the obstacles that have a bad effect on the enhancement of the energy storage capability;

Thus, it is vital to develop facile methods to manufacture $NiCo_2O_4$ electrodes with excellent pseudocapacitive performance of high loading mass of active materials (more than 10 mg cm^{-2}), which are seriously pursued by commercial application.

As the nature of semiconductor, it is imperative to further improve its conductivity by incorporating other materials with good electrical conductivity or by depositing onto conductive substrates with good contact. Furthermore, as the morphologies of electrode materials have a substantial influence on the speed of ion transfer and the capacity of charge storage, it is crucial to synthesize materials with excellent morphology. We do hope that novel nanostructures, such as hollow, core-shell, hollow-core-shell and so forth, can be poured into this field to further improve the electrochemical performances with suitable approaches.

In order to fully exploit the potential of $NiCo_2O_4$-based electrode materials, it is imperative to optimize both synthesis parameters and material properties. The engineering factors of electrodes, including electrolytes, membrane separators, current collectors, counter electrodes and packaging, are not well established in the literature that need a deeper investigation. But we believe that enhanced performances for $NiCo_2O_4$-based supercapacitors will be expected from both fundamental and practical viewpoints in the near future.

Acknowledgements

The work is financially supported by the National Natural Science Foundation of China (51134007, 21003161 and 21250110060), the Distinguished Young Scientists of Hunan Province (13JJ1004), the Program for the New Century Excellent Talents in

University (NCET-11-0513), and the Hunan Provincial Innovation Foundation for Postgraduate (CX2013B048).

References

1 S. Chu and A. Majumdar, nature, 2012, **488**, 294-303.

2 H.-J. Choi, S.-M. Jung, J.-M. Seo, D.W. Chang, L. Dai and J.-B. Baek, Nano Energy, 2012, **1**, 534-551.

3 P. Simon and Y. Gogotsi, Nature materials, 2008, **7**, 845-854.

4 A.S. Aricò, P. Bruce, B. Scrosati and J.-M. Tarascon, W. Van Schalkwijk, Nature materials, 2005, **4**, 366-377.

5 X. Lang, A. Hirata, T. Fujita and M. Chen, Nature Nanotechnology, 2011, **6**, 232-236.

6 J.R. Miller and P. Simon, Science Magazine, 2008, **321**, 651-652.

7 P. Simon, Y. Gogotsi and B. Dunn, Science Magazine, 2014, **343**, 1210-1211.

8 A. Davies and A. Yu, The Canadian Journal of Chemical Engineering, 2011, **89**, 1342-1357.

9 A. Alonso, V. Ruiz, C. Blanco, R. Santamaria, M. Granda, R. Menendez and S. De Jager, Carbon, 2006, **44**, 441-446.

10 E. Frackowiak and F. Beguin, Carbon, 2001, **39**, 937-950.

11 J. Huang, B.G. Sumpter and V. Meunier, Chemistry-A European Journal, 2008, **14**, 6614-6626.

12 W. Wang, S. Guo, M. Penchev, I. Ruiz, K.N. Bozhilov, D. Yan, M. Ozkan and C.S. Ozkan, Nano Energy, 2013, **2**, 294-303.

13 G.A. Snook, P. Kao and A.S. Best, Journal of Power Sources, 2011, **196**, 1-12.

14 G.A. Snook and G.Z. Chen, Journal of Electroanalytical Chemistry, 2008, **612**, 140-146.

15 Z. Lu, Z. Chang, J. Liu and X. Sun, Nano Research, 2011, **4**, 658-665.

16 S.K. Meher, P. Justin and G.R. Rao, Nanoscale, 2011, **3**, 683-692.

17 X. Wang, C. Yan and A. Sumboja, P.S. Lee, Nano Energy, 2014, **3**, 119-126.

18 V. Anisimov, M. Korotin and E. Kurmaev, Journal of Physics: Condensed Matter, 1990, **2**, 3973-3987.

19 C. Yuan, J. Li, L. Hou, J. Lin, X. Zhang and S. Xiong, Journal of Materials Chemistry A, 2013, **1**, 11145-11151.

20 R. Memming, Processes at semiconductor electrodes, Comprehensive treatise of electrochemistry, Springer1983, 529-592.

21 C.-C. Hu, K.-H. Chang, M.-C. Lin and Y.-T. Wu, Nano Letters, 2006, **6**, 2690-2695.

22 H. Xia, Y.S. Meng, G. Yuan, C. Cui and L. Lu, Electrochemical and solid-state letters, 2012, **15**, A60-A63.

23 C. Yuan, X. Zhang, L. Su, B. Gao and L. Shen, Journal of Materials Chemistry, 2009, **19**, 5772-5777.

24 W. Wen, J.-M. Wu and M.-H. Cao, Nano Energy, 2013, **2**, 1383-1390.

25 S. Xiong, C. Yuan, X. Zhang and B. Xi, Y. Qian, Chemistry-A European Journal, 2009, **15**, 5320-5326.

26 X.-h. Xia, J.-p. Tu, Y.-j. Mai, X.-l. Wang, C.-d. Gu and X.-b. Zhao, Journal of Materials Chemistry, 2011, **21**, 9319-9325.

27 S. Chen, J. Zhu, X. Wu, Q. Han and X. Wang, ACS Nano, 2010, **4**, 2822-2830.

28 M. Liu, W.W. Tjiu, J. Pan, C. Zhang, W. Gao and T. Liu, Nanoscale, 2014, **6**, 4233-4242.

29 C.-C. Hu and W.-C. Chen, Electrochimica Acta, 2004, **49**, 3469-3477.

30 W. Deng, X. Ji, Q. Chen and C.E. Banks, RSC Advances, 2011, **1**, 1171-1178.

31 T. Cottineau, M. Toupin, T. Delahaye, T. Brousse and D. Belanger, Applied Physics A, 2006, **82**, 599-606.

32 T.Y. Wei, C.H. Chen, H.C. Chien, S.Y. Lu and C.C. Hu, Advanced Materials, 2010, **22**, 347-351.

33 X. Wang, W.S. Liu, X. Lu and P.S. Lee, Journal of Materials Chemistry, 2012, **22**, 23114-23119.

34 Y. Li, P. Hasin and Y. Wu, Advanced Materials, 2010, **22**, 1926-1929.

35 H. Chen, J. Jiang, L. Zhang, T. Qi, D. Xia and H. Wan, Journal of Power Sources, 2014, **248**, 28-36.

36 C. Yuan, J. Li, L. Hou, X. Zhang, L. Shen and X.W.D. Lou, Advanced Functional Materials, 2012, **22**, 4592-4597.

37 B. Cui, H. Lin, J.B. Li, X. Li and J. Yang, J. Tao, Advanced Functional Materials, 2008, **18**, 1440-1447.

38 H. Jiang, J. Ma and C. Li, Chemical Communications, 2012, **48**, 4465-4467.

39 A.D. Dalvi, W.G. Bacon and R.C. Osborne, PDAC 2004 International Convention, Trade Show & Investors Exchange, Toronto: The prospectors and Developers Association of Canada, 2004, 1-27.

40 J. Reid and Nickel, 1996, **96**, 11-16.

41 X. Wang, W. Tian, T. Zhai, C. Zhi, Y. Bando and D. Golberg, Journal of Materials Chemistry, 2012, **22**, 23310-23326.

42 W. Wei, X. Cui, W. Chen and D.G. Ivey, Chemical Society Reviews, 2011, **40**, 1697-1721.

43 R.S. Devan, R.A. Patil, J.H. Lin and Y.R. Ma, Advanced Functional Materials, 2012, **22**, 3326-3370.

44 G. Wang, L. Zhang and J. Zhang, Chemical Society Reviews, 2012, **41**, 797-828.

45 B. Cui, H. Lin, Y.-z. Liu, J.-b. Li, P. Sun, X.-c. Zhao and C.-j. Liu, The Journal of Physical Chemistry C, 2009, **113**, 14083-14087.

46 J. Marco, J. Gancedo, M. Gracia, J. Gautier, E. Rıos and F. Berry, Journal of Solid State Chemistry, 2000, **153**, 74-81.

47 J.-G. Kim, D. Pugmire, D. Battaglia and M. Langell, Applied surface science, 2000, **165**, 70-84.

48 O. Knop, K. Reid, Sutarno and Y. Nakagawa, Canadian Journal of Chemistry, 1968, **46**, 3463-3476.

49 M. Lenglet, R. Guillamet, J. Dürr, D. Gryffroy and R. Vandenberghe, Solid State Communications, 1990, **74**, 1035-1039.

50 C.-T. Hsu, C.-C. Hu and Journal of Power Sources, 2013, **242**, 662-671.

51 R.W. Grimes, A.B. Anderson and A.H. Heuer, Journal of the American Chemical Society, 1989, **111**, 1-7.

52 X. Liu, S. Shi, Q. Xiong, L. Li, Y. Zhang, H. Tang, C. Gu, X. Wang and J. Tu, ACS Applied Materials & Interfaces, 2013, **5**, 8790-8795.

53 Y. Chen, B. Qu, L. Hu, Z. Xu, Q. Li and T. Wang, Nanoscale, 2013, **5**, 9812-9820.

54 J. Haenen, W. Visscher and E. Barendrecht, Journal of Electroanalytical Chemistry and Interfacial Electrochemistry, 1986, **208**, 273-296.

55 P. Rasiyah, A. Tseung and D. Hibbert, Journal of The Electrochemical Society, 1982, **129**, 1724-1727.

56 C. An, Y. Wang, Y. Huang, Y. Xu, C. Xu, L. Jiao and H. Yuan, CrystEngComm, 2014, **16**, 385-392.

57 X.-C. Dong, Z. Yufei, M. Mingze, Y. Jun, S. Haiquan and W. Huang, Nanoscale, 2014, **6**, 4303-4308.

58 L.L. Hench and J.K. West, Chemical Reviews, 1990, **90**, 33-72.

59 M. Niederberger, Accounts of chemical research, 2007, **40**, 793-800.

60 J. Livage, M. Henry and C. Sanchez, Progress in Solid State Chemistry, 1988, **18**, 259-341.

61 L.-B. Kong, C. Lu, M.-C. Liu, Y.-C. Luo and L. Kang, Journal of Solid State Electrochemistry, 2013, **17**, 1463-1471.

62 Y.Q. Wu, X.Y. Chen, P.T. Ji and Q.Q. Zhou, Electrochimica Acta, 2011, **56**, 7517-7522.

63 M.-C. Liu, L.-B. Kong, C. Lu, X.-M. Li, Y.-C. Luo and L. Kang, ACS Applied Materials & Interfaces, 2012, **4**, 4631-4636.

64 M.-C. Liu, L.-B. Kong, C. Lu, X.-M. Li, Y.-C. Luo, L. Kang, X. Li and F.C. Walsh, Journal of The Electrochemical Society, 2012, **159**, A1262-A1266.

65 G. Hu, C. Tang, C. Li, H. Li, Y. Wang and H. Gong, Journal of The Electrochemical Society, 2011, **158**, A695-A699.

66 S. Feng and R. Xu, Accounts of chemical research, 2001, **34**, 239-247.

67 K. Byrappa and T. Adschiri, Progress in Crystal Growth and Characterization of Materials, 2007, **53**, 117-166.

68 R. Zou, K. Xu, T. Wang, G. He, Q. Liu, X. Liu, Z. Zhang and J. Hu, Journal of Materials Chemistry A, 2013, **1**, 8560-8566.

69 X. Liu, Y. Zhang, X. Xia, S. Shi, Y. Lu, X. Wang, C. Gu and J. Tu, Journal of Power Sources, 2013, **239**, 157-163.

70 X. Wang, X. Han, M. Lim, N. Singh, C.L. Gan, M. Jan and P.S. Lee, The Journal of Physical Chemistry C, 2012, **116**, 12448-12454.

71 L. Shen, Q. Che, H. Li and X. Zhang, Advanced Functional Materials, 2014, **24**, 2630-2637

72 G. Zhang and X.W.D. Lou, Scientific Reports, 2013, **3**, 1470.

73 M. Musiani, Electrochimica Acta, 2000, **45**, 3397-3402.

74 G. Zhang, T. Wang, X. Yu, H. Zhang, H. Duan and B. Lu, Nano Energy, 2013, **2**, 586-594.

75 L. Huang, D. Chen, Y. Ding, Z.L. Wang, Z. Zeng and M. Liu, ACS Applied Materials & Interfaces, 2013, **5**, 11159-11162.

76 Y.-M. Wang, X. Zhang, C.-Y. Guo, Y.-Q. Zhao, C.-L. Xu and H.-L. Li, Journal of Materials

Chemistry A, 2013, **1**, 13290-13300.

77 J. Du, G. Zhou, H. Zhang, C. Cheng, J. Ma, W. Wei, L. Chen and T. Wang, ACS Applied Materials & Interfaces, 2013, **5**, 7405-7409.

78 X.-F. Lu, D.-J. Wu, R.-Z. Li, S.-H. Ye, Q. Li, Y.-X. Tong and G.-R. Li, Journal of Materials Chemistry A, 2014, **2**, 4706-4713.

79 C.-C. Tseng, J.-L. Lee, Y.-M. Liu, M.-D. Ger and Y.-Y. Shu, Journal of the Taiwan Institute of Chemical Engineers, 2013, **44**, 415-419.

80 C.-C. Hu, C.-T. Hsu, K.-H. Chang and H.-Y. Hsu, Journal of Power Sources, 2013, **238**, 180-189.

81 C. Yuan, J. Li, L. Hou, J. Lin, G. Pang, L. Zhang, L. Lian and X. Zhang, RSC Advances, 2013, **3**, 18573-18578.

82 R. Ding, L. Qi, M. Jia and H. Wang, Journal of Applied Electrochemistry, 2013, **43**, 903-910.

83 N. Padmanathan and S. Selladurai, American Institute of Physics Conference Series, 2013, 1216-1217.

84 R.R. Salunkhe, K. Jang, H. Yu, S. Yu, T. Ganesh and S.-H. Han, H. Ahn, Journal of Alloys and Compounds, 2011, **509**, 6677-6682.

85 S.-K. Chang, K.-T. Lee, Z. Zainal, K.-B. Tan, N.A. Yusof, W.M.D.W. Yusoff, J.-F. Lee and N.-L. Wu, Electrochimica Acta, 2012, **67**, 67-72.

86 I. Shakir, M. Sarfraz, U.A. Rana, M. Nadeem and M.A. Al-Shaikh, RSC Advances, 2013, **3**, 21386-21389.

87 L. Li, S. Peng, Y. Cheah, P. Teh, J. Wang, G. Wee, Y. Ko, C. Wong and M. Srinivasan, Chemistry-A European Journal, 2013, **19**, 5892-5898.

88 Y. Zhao and L. Jiang, Advanced Materials, 2009, **21**, 3621-3638.

89 G. Zhang and X.W.D. Lou, Advanced Materials, 2013, **25**, 976-979.

90 H. Jiang, P.S. Lee and C. Li, Energy & Environmental Science, 2013, **6**, 41-53.

91 N. Padmanathan and S. Selladurai, RSC Advances, 2014, **4**, 8341-8349.

92 Q. Lu, Y. Chen, W. Li, J.G. Chen, J.Q. Xiao and F. Jiao, Journal of Materials Chemistry A, 2013, **1**, 2331-2336.

93 C. Yuan, J. Li, L. Hou, L. Yang, L. Shen and X. Zhang, Journal of Materials Chemistry, 2012, **22**, 16084-16090.

94 Q. Wang, X. Wang, B. Liu, G. Yu, X. Hou, D. Chen and G. Shen, Journal of Materials Chemistry A, 2013, **1**, 2468-2473.

95 H.C. Chien, W.Y. Cheng, Y.H. Wang and S.Y. Lu, Advanced Functional Materials, 2012, **22**, 5038-5043.

96 H. Wang, C.M. Holt, Z. Li, X. Tan, B.S. Amirkhiz, Z. Xu, B.C. Olsen, T. Stephenson and D. Mitlin, Nano Research, 2012, **5**, 605-617.

97 D. Carriazo, J. Patiño, M.C. Gutiérrez, M.L. Ferrer and F. del Monte, RSC Advances, 2013, **3**, 13690-13695.

98 L. Wang, X. Wang, X. Xiao, F. Xu, Y. Sun and Z. Li, Electrochimica Acta, 2013, **111**, 937-945.

99 L. Yu, G. Zhang, C. Yuan and X.W.D. Lou, Chemical Communications, 2013, **49**, 137-139.

100 W. Yang, Z. Gao, J. Ma, X. Zhang, J. Wang and J. Liu, Journal of Materials Chemistry A, 2014, **2**, 1448-1457.

101 L. Huang, D. Chen, Y. Ding, S. Feng, Z.L. Wang and M. Liu, Nano Letters, 2013, **13**, 3135-3139.

102 Q. Wang, B. Liu, X. Wang, S. Ran, L. Wang, D. Chen and G. Shen, Journal of Materials Chemistry, 2012, **22**, 21647-21653.

103 H.-Y. WU and H.-W. WANG, Acta Physico-Chimica Sinica, 2013, **29**, 1501-1506.

104 R. Ding, L. Qi, M. Jia and H. Wang, Electrochimica Acta, 2013, **107**, 494-502.

105 P.D. Cai, B. Liu, D. Wang, L. Wang, Y. Liu, H. Li, Y. Wang, Q. Li and T. Wang, Journal of Materials Chemistry A, 2014, **2**, 4954-4960.

106 C. Qian, Z. Fang, Z. Xiao-Gang, L. Xiang-Jun, D. Bing and Z. Jia-Jia, Acta Physico-Chimica Sinica, 2012, **28**, 837-842.

107 K. Xu, W. Li, Q. Liu, B. Li, X. Liu, L. An, Z. Chen, R. Zou and J. Hu, J. Mater. Chem. A, 2014, **2**, 4795-4802.

Table captions

Table 1. Morphology, synthetic method and specific capacitance of $NiCo_2O_4$ electrodes

Table 2. Morphology, synthetic method and specific capacitance of $NiCo_2O_4$-based composite electrodes

Table 1

Morphology	Synthetic method	Specific capacitance	Load mass /mg cm^{-2}	Ref.
$NiCo_2O_4$ nanowire arrays	Hydrothermal	2681 F g^{-1} (2 A g^{-1})	3	94
$NiCo_2O_4$ nanorods	Chemical bath deposition	490 F g^{-1}	＞0.3	84
$NiCo_2O_4$ nanosheets	Chemical bath deposition	330 F g^{-1}	＞0.3	84
$NiCo_2O_4$ nanotubes	Electrospinning	1647 F g^{-1} (1 A g^{-1})	/	87
$NiCo_2O_4$ aerogels	Sol-gel	1400 F g^{-1}(25mV s^{-1})	0.4	32
$NiCo_2O_4$ nanoflakes	Hydrothermal	844 F g^{-1} (1 A g^{-1})	0.0625	91
$NiCo_2O_4$ nanowall-network	Hydrothermal	1225 F g^{-1} (5 A g^{-1})	0.0625	91
$NiCo_2O_4$ nanoflake@nanowire	Hydrothermal	891 F g^{-1} (1 A g^{-1})	1.8	69
Urchin-like $NiCo_2O_4$	Hydrothermal	1650 F g^{-1} (1 A g^{-1})	/	102
Chain-like $NiCo_2O_4$ nanowires	Hydrothermal	1284 F g^{-1} (2 A g^{-1})	/	68
Pine-like $NiCo_2O_4$	Hydrothermal	2132 F g^{-1}(10 A g^{-1})	1.8	53
Hierarchical porous network-like $NiCo_2O_4$	Polymer-assisted solution route	587 F g^{-1} (2 A g^{-1})	5	19
Flower-like $NiCo_2O_4$	Solvothermal	1191 F g^{-1} (1 A g^{-1})	/	35
Hierarchial $NiCo_2O_4$@$NiCo_2O_4$ core/shell nanoflake	Hydrothermal and chemical bath deposition	787 F g^{-1} (1 A g^{-1})	1.97	52
Mesoporous $NiCo_2O_4$ nanosheets	Co-electrodeposition	2010 F g^{-1} (2 A g^{-1})	0.8	36
Mesoporous $NiCo_2O_4$ nanowires	Template-free	401 F g^{-1} (1 A g^{-1})	8.5	93
Uniform mesoporous hollow $NiCo_2O_4$ sub-microspheres	Template-engaged	678 F g^{-1} (1 A g^{-1})	8	81
Ordered mesoporous $NiCo_2O_4$	Hard-template method	612 F g^{-1} (28.6 A g^{-1})	＞10	92
Mesoporous $NiCo_2O_4$ nanosheets	General solution method	1743 F g^{-1} (7.08 A g^{-1})	1.2	89

Table 2

Morphology	Synthetic method	Specific capacitance	Load mass /mg cm^{-2}	Ref.
Ultrathin porous $NiCo_2O_4$ nanosheet@flexible carbon fabric	Co-electrodeposition	2658 F g^{-1} (2 A g^{-1})	0.6	77
$NiCo_2O_4$@carbon aerogel	Two-step wet chemistry process	1700 F g^{-1} (25 mV s^{-1})	0.23	95
$NiCo_2O_4$ nanorods@carbon nanofibers	Facile solution method	1023.6 F g^{-1} (1 A g^{-1})	/	72
$NiCo_2O_4$ nanosheets@carbon nanofibers	Facile solution method	1002 F g^{-1} (1 A g^{-1})	/	72
$NiCo_2O_4$@single wall carbon nanotube	Controlled hydrolysis process	1642 F g^{-1} (0.5 A g^{-1})	3	70
Nanoforest of hierarchical Co_3O_4@$NiCo_2O_4$ nanowire arrays	Co-electrodeposition	526.7 F g^{-1} (20 A g^{-1})	1.5	74
$Ni(OH)_2$ nanosheets@$NiCo_2O_4$ nanosheets	Co-electrodeposition	3250 F g^{-1} (1.25 A g^{-1})	1.6	75
$NiCo_2O_4$ nanoflower@activated carbon fiber	Hydrothermal	1626 F g^{-1} (1 A g^{-1})	2.4	103
Activated carbon@ $NiCo_2O_4$	Chemical synthesis	351 F g^{-1} (1 A g^{-1})	4	104
$NiCo_2O_4$@graphene	Hydrolysis	618 F g^{-1}(5 mV s^{-1})	10	96
$NiCo_2O_4$@graphene oxide	Microwave-assisted	925 F g^{-1} (1.5 A g^{-1})	4	97
$NiCo_2O_4$ nanoflake@reduced graphene oxide	Situ assembling	1693 F g^{-1} (1 A g^{-1})	2	98
Hierarchical $NiCo_2O_4$@MnO_2 core–shell heterostructured nanowire arrays	Two-step solution route	1603 F g^{-1} (1.43 A g^{-1})	1.4	99
Hierarchical $NiCo_2O_4$@NiO core–shell heterostructured nanowire arrays	A simple process	1792 F g^{-1} (4.2 A g^{-1})	1.19	100
$NiCo_2O_4$ nanowires@$CoMoO_4$ nanoplates core/shell nanowire arrays	Hydrothermal	1005 F g^{-1} (0.685 A g^{-1})	14.6	105
NiO@$NiCo_2O_4$@Co_3O_4	Sol-gel	1717 F g^{-1} (0.625 A g^{-1})	8	63
$Co_{0.67}Ni_{0.33}$DHs nanosheets @$NiCo_2O_4$ nanowires	Hydrothermal and electrodeposition	1640 F g^{-1} (2 A g^{-1})	1	101
Mesoporous $NiCo_2O_4$ nanowire arrays@carbon textiles	Hydrothermal	1283 F g^{-1} (1 A g^{-1})	1.2	71
Ordered mesoporous carbon @$NiCo_2O_4$	Co-precipitation	577 F g^{-1} (1 A g^{-1})	/	106

Figure caption

Figure 1. I-V curves of the $NiCo_2O_4$, NiO and Co_3O_4 samples. Reprinted from Ref. 35 with permission. Copyright 2013, Elsevier B.V.

Figure 2. Ragone plot of the current electrochemical performance for $NiCo_2O_4$-based asymmetric supercapacitors. Reprinted from Ref. 107 with permission. Copyright 2014, The Royal Society of Chemistry; Reprinted from Ref. 78 with permission. Copyright 2014, The Royal Society of Chemistry; Reprinted from Ref. 50 with permission. Copyright 2013, Elsevier B.V; Reprinted from Ref. 33 with permission. Copyright 2012, The Royal Society of Chemistry; Reprinted from Ref. 35 with permission. Copyright 2013, Elsevier B.V; Reprinted from Ref. 104 with permission. Copyright 2013, Elsevier Ltd; Reprinted from Ref. 96 with permission. Copyright 2012, Tsinghua University Press and Springer-Verlag Berlin Heidelberg.

Figure 3. Spinel structure of $NiCo_2O_4$ unit cell. Reprinted from Ref. 102 with permission. Copyright 2012, The Royal Society of Chemistry.

Figure 4. Schematic of charge storage mechanism of $NiCo_2O_4$

Figure 5. Typical synthetic processes of $NiCo_2O_4$.

Figure 6. (a) Scheme of the products at various reaction stages; (b) Proposed mechanism for the effect of NH_4F on morphology construction. Reprinted from Ref. 53 with permission. Copyright 2013, The Royal Society of Chemistry.

Figure 7. Illustration of the formation process of $Co_3O_4@NiCo_2O_4$ NWFAs hierarchical heterostructures. (a) Ni-foam substrate; (b) Hydrothermal synthesis of aligned Co_3O_4 nanowire arrays; (c) Formation of hierarchical $Co_3O_4@NiCo_2O_4$ nanoflake arrays via a co-electrodeposition process. Reprinted from Ref. 74 with permission. Copyright 2013, Elsevier Ltd.

Figure 8. Assemblies of $NiCo_2O_4$-based materials with different morphologies and various combinations of novel nanomaterials.

Figure 9. (a–c) TEM and (d) Schematic illustration of the charge storage advantages of the 3D hierarchical porous network-like $NiCo_2O_4$ framework electrode. Reprinted from Ref. 19 with permission. Copyright©2013, The Royal Society of Chemistry.

Figure 10. (a, b) TEM images of ordered mesoporous $NiCo_2O_4$. Reprinted from Ref. 82 with permission. Copyright 2013, The Royal Society of Chemistry. (c, d) FESEM images of $NiCo_2O_4$ nanowire arrays grown on Ni foams. Reprinted from Ref. 94 with permission. Copyright 2013, The Royal Society of Chemistry.

Figure 11. (a, b) SEM images of carbon aerogel and $NiCo_2O_4$/carbon aerogel composite, respectively; (c, d) HAADF and HRTEM images of $NiCo_2O_4$/carbon aerogel composite, respectively. Reprinted from Ref. 95 with permission. Copyright 2012, WILEY-VCH Verlag GmbH & Co. KGaA, Weinheim.

Figure 12. (a, b) SEM and (c, d) TEM images of the final $NiCo_2O_4$@NiO/CC product at different magnifications (the inset of (d) is its HRTEM image). Reprinted from Ref. 100 with permission . Copyright 2014, The Royal Society of Chemistry.

Figure 13. (a) SEM image of CFP before (inset) and after growth of $NiCo_2O_4$ nanowires; (b) High-magnification SEM image of $NiCo_2O_4$ nanowires grown on CFP; (c) TEM image and HRTEM image (inset) of 2 $NiCo_2O_4$ nanowires; (d) Diffraction pattern of a $NiCo_2O_4$ nanowire. (e) SEM image of a CoDHs coating on $NiCo_2O_4$ nanowire grown on CFP; (f) TEM image of CoDHs/$NiCo_2O_4$ nanowires grown on CFP. Reprinted from Ref. 101 with permission. Copyright 2013, American Chemical Society.

Figure 14. (a) Specific energy and power density of $Co_xNi_{1-x}DH_n/NiCo_2O_4$/CFP electrodes evaluated at different charge/discharge rates (current densities); (1) CoDHs/$NiCo_2O_4$/CFP; (2) $Co_{0.67}Ni_{0.33}$DHs/$NiCo_2O_4$/CFP; (3) $Co_{0.5}Ni_{0.5}$DHs/$NiCo_2O_4$/CFP; (4) $Co_{0.33}Ni_{0.67}$DHs/$NiCo_2O_4$/CFP. (b) Capacity retention of the hybrid composite electrodes evaluated at a constant charge/discharge cycling rate of 2 mA cm^{-2}. Reprinted from Ref. 101 with permission. Copyright 2013, American Chemical Society.

Figure 1.

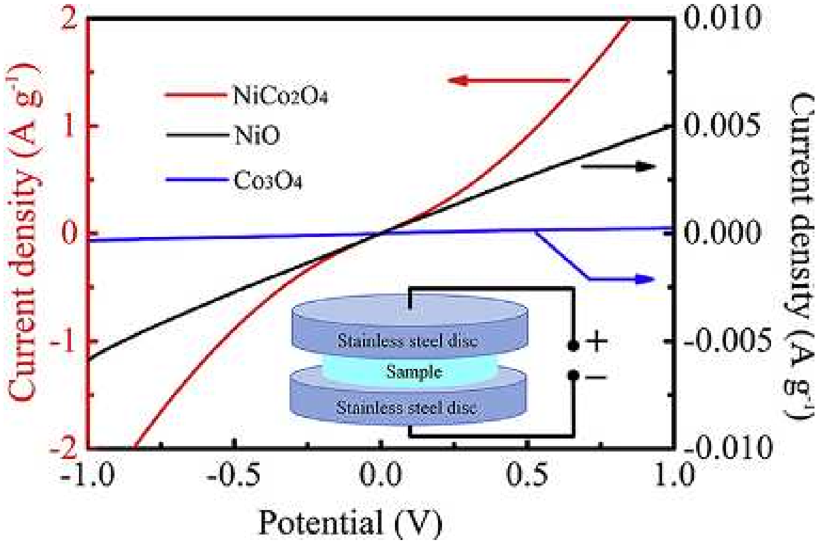
Current density (A g^{-1})
2
1
0
-1
-2
NiCo$_2$O$_4$
NiO
Co$_3$O$_4$
Stainless steel disc
Sample
Stainless steel disc
+
−
0.010
0.005
0.000
-0.005
-0.010
Current density (A g^{-1})
-1.0
-0.5
0.0
0.5
1.0
Potential (V)

Figure 2.

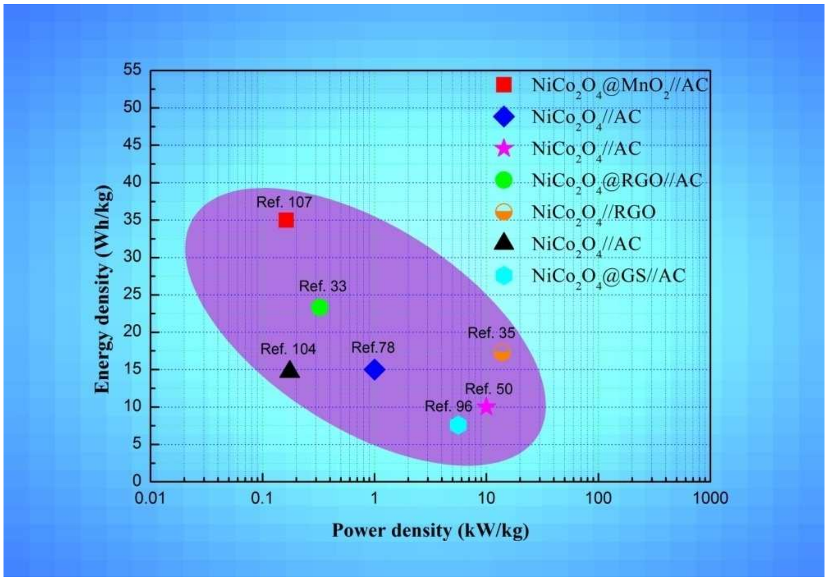
Energy density (Wh/kg)
0
5
10
15
20
25
30
35
40
45
50
55
Power density (kW/kg)
0.01
0.1
1
10
100
1000
Ref. 107
Ref. 33
Ref. 104
Ref.78
Ref. 35
Ref. 50
Ref. 96
$NiCo_2O_4@MnO_2//AC$
$NiCo_2O_4//AC$
$NiCo_2O_4//AC$
$NiCo_2O_4@RGO//AC$
$NiCo_2O_4//RGO$
$NiCo_2O_4//AC$
$NiCo_2O_4@GS//AC$

Figure 3.

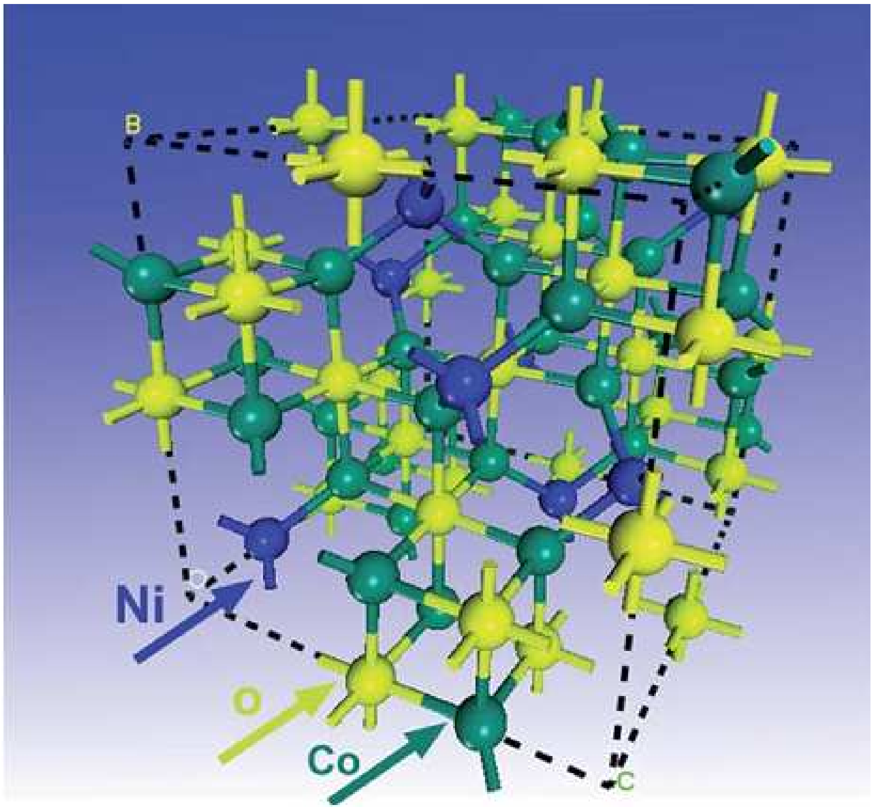

Figure 4.

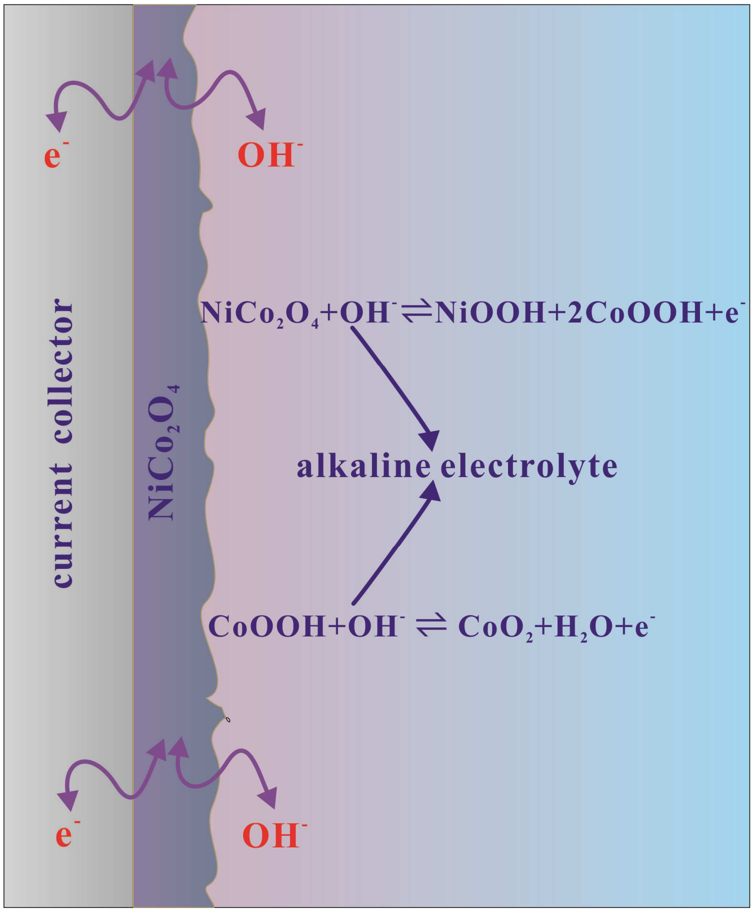
e$^-$
OH$^-$
current collector
$NiCo_2O_4$
$NiCo_2O_4+OH^- \rightleftharpoons NiOOH+2CoOOH+e^-$
alkaline electrolyte
$CoOOH+OH^- \rightleftharpoons CoO_2+H_2O+e^-$
e$^-$
OH$^-$

Figure 5.

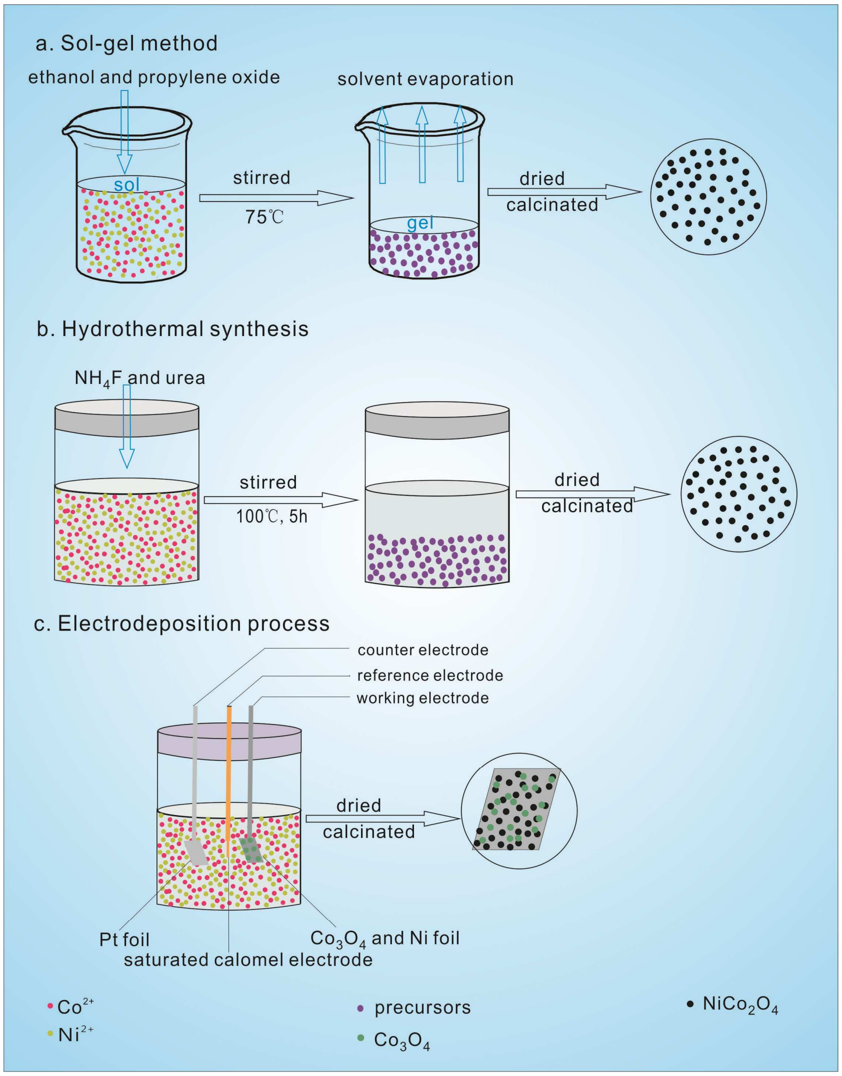
a. Sol-gel method
ethanol and propylene oxide
solvent evaporation
sol
stirred
75℃
gel
dried
calcinated
b. Hydrothermal synthesis
NH$_4$F and urea
stirred
100℃, 5h
dried
calcinated
c. Electrodeposition process
counter electrode
reference electrode
working electrode
dried
calcinated
Pt foil
Co$_3$O$_4$ and Ni foil
saturated calomel electrode
Co^{2+}
Ni^{2+}
precursors
Co$_3$O$_4$
NiCo$_2$O$_4$

Figure 6.

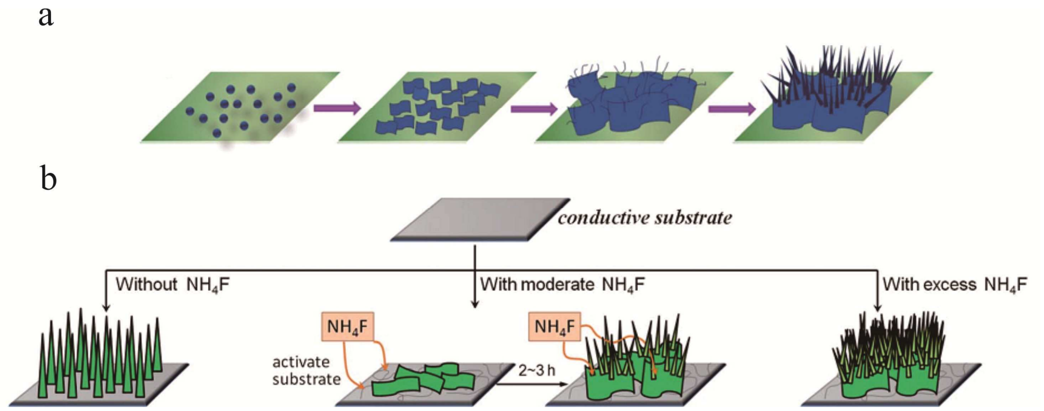
a
b
conductive substrate
Without NH$_4$F
With moderate NH$_4$F
With excess NH$_4$F
NH$_4$F
activate substrate
2~3 h
NH$_4$F

Figure 7.

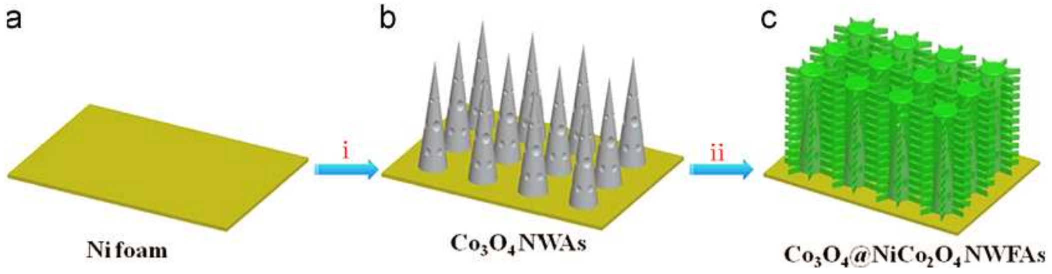

Figure 8.

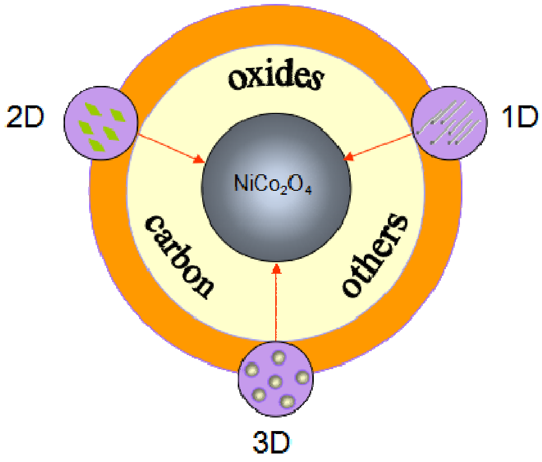

Figure 9.

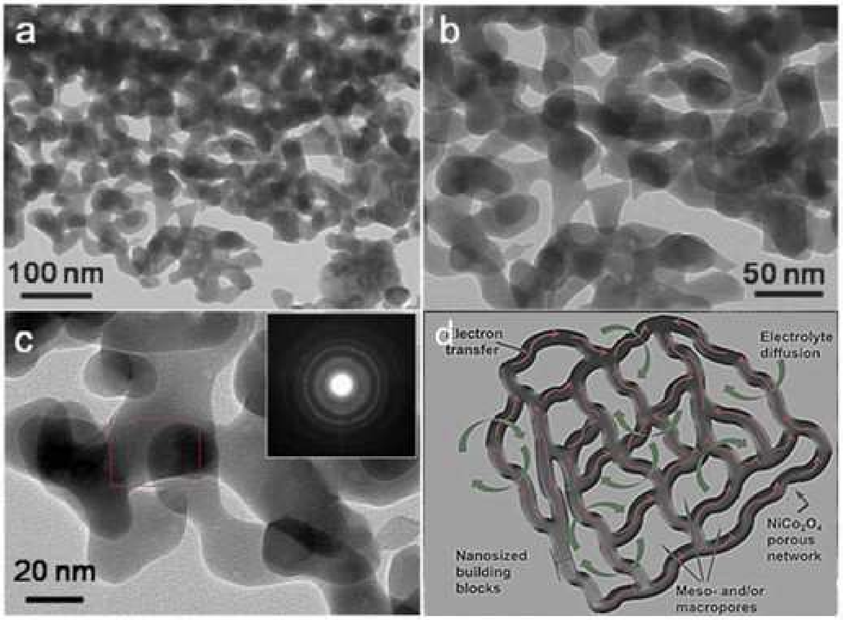
a
100 nm
b
50 nm
c
20 nm
d
Electron transfer
Electrolyte diffusion
$NiCo_2O_4$ porous network
Nanosized building blocks
Meso- and/or macropores

Figure 10.

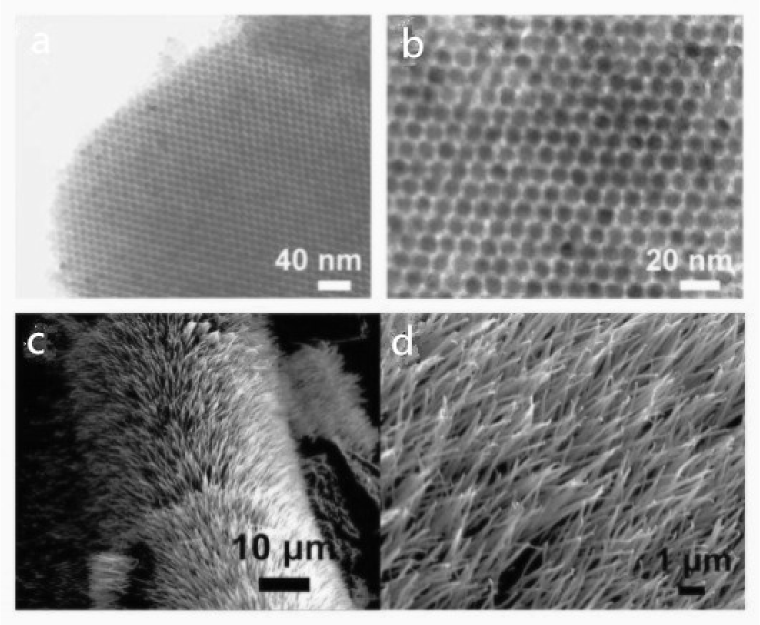

Figure 11.

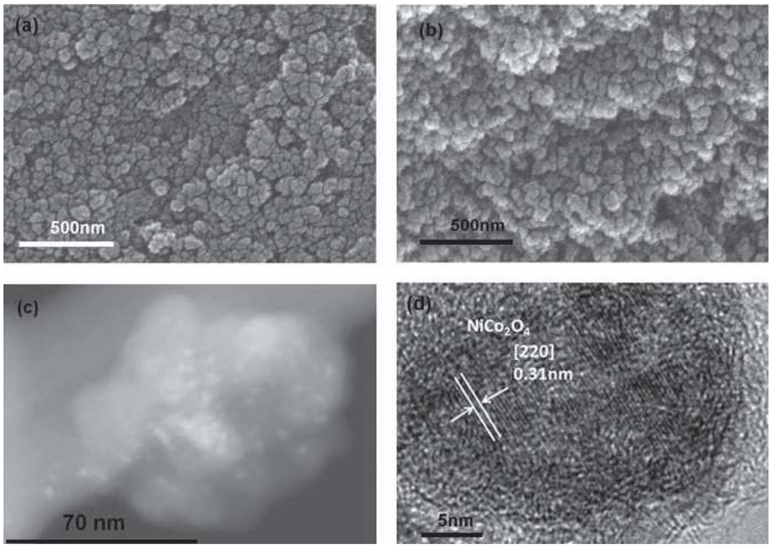

Figure 12.

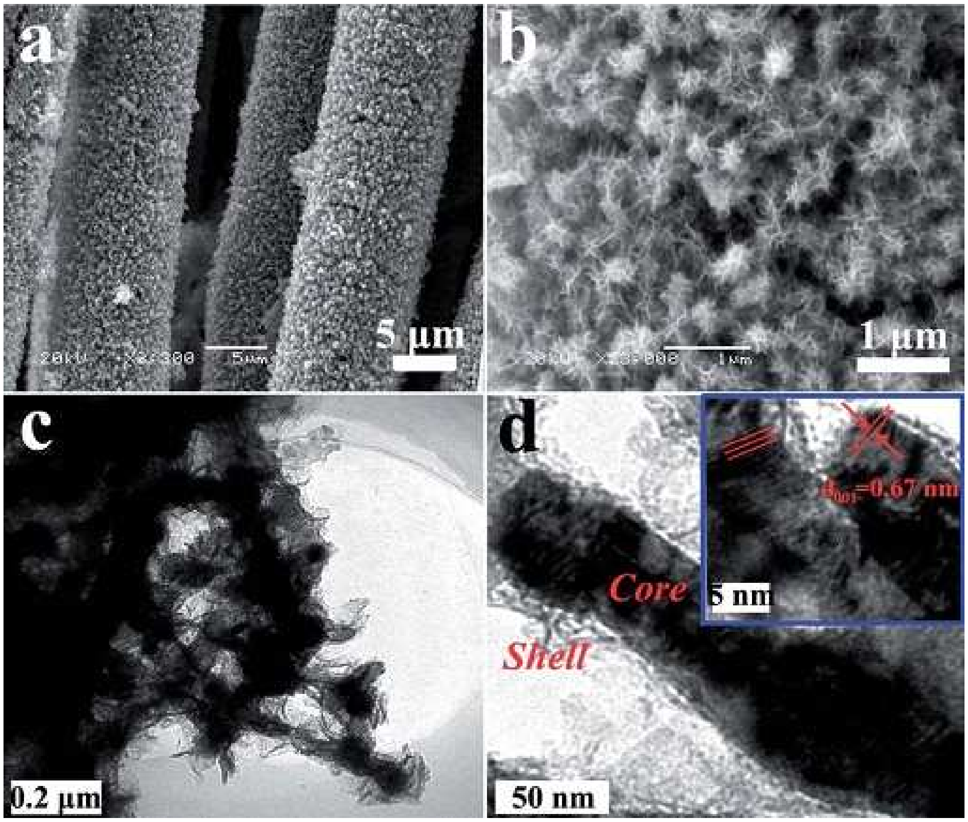

Figure 13.

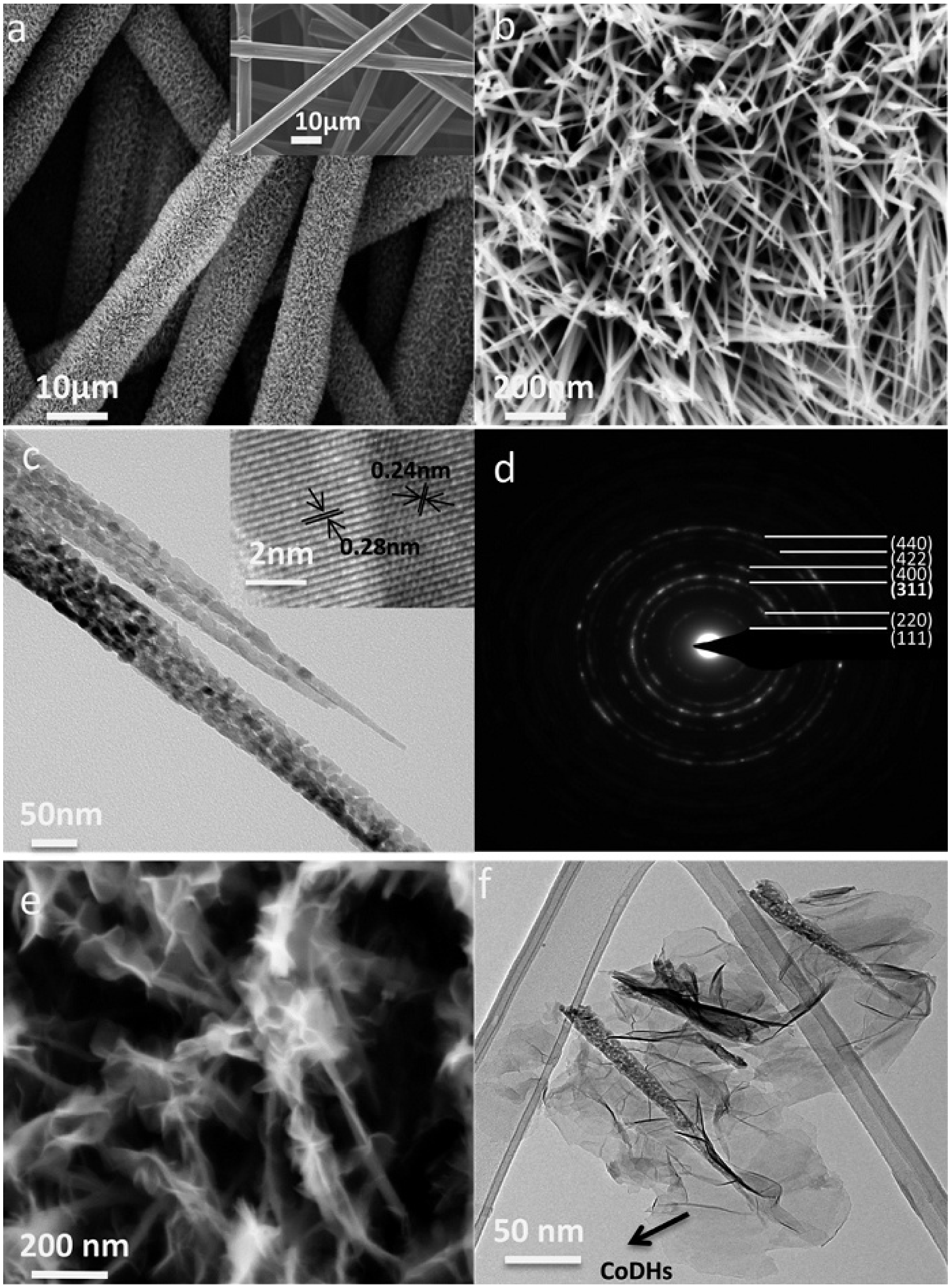
a
10μm
10μm
b
200nm
c
0.24nm
2nm
0.28nm
50nm
d
(440)
(422)
(400)
(311)
(220)
(111)
e
200 nm
f
50 nm
CoDHs

Figure 14.

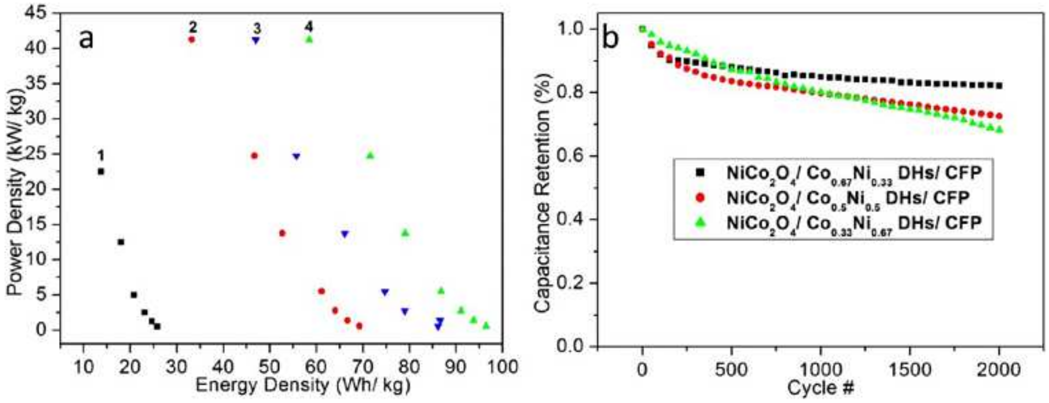
a
Power Density (kW/ kg)
Energy Density (Wh/ kg)
0
5
10
15
20
25
30
35
40
45
10
20
30
40
50
60
70
80
90
100
1
2
3
4
b
Capacitance Retention (%)
Cycle #
0.0
0.2
0.4
0.6
0.8
1.0
0
500
1000
1500
2000
■ $NiCo_2O_4$/ $Co_{0.67}Ni_{0.33}$ DHs/ CFP
● $NiCo_2O_4$/ $Co_{0.5}Ni_{0.5}$ DHs/ CFP
▲ $NiCo_2O_4$/ $Co_{0.33}Ni_{0.67}$ DHs/ CFP

Graphical abstract